BIOCHEMISTRY
including biophysical chemistry & molecular biology

Article

pubs.acs.org/biochemistry

Protein−Protein Interactions and Substrate Channeling in Orthologous and Chimeric Aldolase−Dehydrogenase Complexes

Perrin Baker, Colleen Hillis, Jason Carere, and Stephen Y. K. Seah*

Department of Molecular and Cellular Biology, University of Guelph, Guelph, Ontario, Canada

Supporting Information

ABSTRACT: Bacterial aldolase−dehydrogenase complexes catalyze the last steps in the *meta* cleavage pathway of aromatic hydrocarbon degradation. The aldolase (TTHB246) and dehydrogenase (TTHB247) from *Thermus thermophilus* were separately expressed and purified from recombinant *Escherichia coli*. The aldolase forms a dimer, while the dehydrogenase is a monomer; these enzymes can form a stable tetrameric complex in vitro, consisting of two aldolase and two dehydrogenase subunits. Upon complex formation, the K_m value of 4-hydroxy-2-oxopentanoate, the substrate of TTHB246, is decreased 4-fold while the K_m of acetaldehyde, the substrate of TTHB247, is increased 3-fold. The k_{cat} values of each enzyme were reduced by ∼2-fold when they were in a complex. The half-life of TTHB247 at 50 °C increased by ∼4-fold when it was in a complex with TTHB246. The acetaldehyde product from TTHB246 could be efficiently channelled directly to TTHB247, but the channeling efficiency for the larger propionaldehyde was ∼40% lower. A single A324G substitution in TTHB246 increased the channeling efficiency of propionaldehyde to a value comparable to that of acetaldehyde. Stable and catalytically competent chimeric complexes could be formed between the *T. thermophilus* enzymes and the orthologous aldolase (BphI) and dehydrogenase (BphJ) from the biphenyl degradation pathway of *Burkholderia xenovorans* LB400. However, channeling efficiencies for acetaldehyde in these chimeric complexes were ∼10%. Structural and sequence analysis suggests that interacting residues in the interface of the aldolase−dehydrogenase complex are highly conserved among homologues, but coevolution of partner enzymes is required to fine-tune this interaction to allow for efficient substrate channeling.

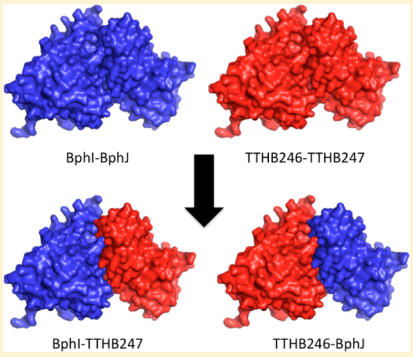

Protein−protein interactions are important in biological systems as they form the core of fundamental cellular processes such as signal transduction, gene expression, and metabolism.[1−3] For example, the formation of multienzyme complexes allows the coordination and regulation of individual enzymes, which has direct bearing on overall catalytic efficiencies and specificities. Several enzyme complexes that catalyze successive reactions in metabolic pathways can also directly transfer common intermediates from one active site to another without release to the bulk solvent.[4] This process, known as substrate channeling, sequesters labile or toxic intermediates, preventing formation of unwanted products from competing cellular reactions, and increases the efficiency of the overall reaction.[5−7]

Aldolase−dehydrogenase complexes in bacterial aromatic *meta* cleavage pathways are examples of bifunctional enzyme complexes that exhibit substrate channeling. The best-characterized complex is BphI−BphJ from the polychlorinated biphenyl (PCB) pollutant degradation pathway in *Burkholderia xenovorans* LB400.[8,9] The class II pyruvate aldolase BphI uses Mn^{2+} as a cofactor to catalyze the reversible C−C bond cleavage of 4-hydroxy-2-oxoacids to form pyruvate and an aldehyde up to six carbons in length.[10−12] The latter product is channelled through a molecular tunnel to the dehydrogenase, BphJ, where it is converted to an acyl-CoA, using CoA and NAD^+ as cofactors.[10] Replacement of two glycines (Gly-322 and Gly-323) that line part of the tunnel with bulkier amino acids led to reduction or abolishment of aldehyde channeling.[13] The aldol cleavage reaction performed by BphI is allosterically activated 15-fold by the dehydrogenase, BphJ, when it undergoes turnover and approximately 4-fold in the presence of the dehydrogenase cofactor, NADH.[10] Because aldehydes are reactive and toxic, substrate channeling and allosteric activation allow for the coupling of the respective enzyme activities and the sequestration of this toxic metabolite from vital cellular macromolecules.

Studies of protein−protein interactions within the aldolase−dehydrogenase complex have been hampered by the inability to separately express BphI, BphJ, or other orthologues in heterologous hosts.[10,14,15] To date, only SanM and SanN from *Streptomyces ansochromogenes*, the aldolase and dehydrogenase involved in nikkomycin biosynthesis,[16] respectively, have been successfully expressed independently in *Streptomyces lividans*. Limited biochemical characterization, focusing on deciphering the functions of these enzymes in the nikkomycin biosynthetic pathway, has shown that while the purified dehydrogenase SanN is active, the aldolase, SanM, is not active unless it is in a complex with SanN.[17]

Here we describe the expression, purification, and characterization of an aldolase and dehydrogenase from the thermophilic

Received: December 12, 2011
Revised: February 1, 2012
Published: February 3, 2012

dx.doi.org/10.1021/bi201832a | *Biochemistry* 2012, 51, 1942−1952

bacterium, *Thermus thermophilus* HB8, that is homologous to the BphI−BphJ and SanN−SanM complexes. Unlike the latter enzyme systems, the *T. thermophilus* enzymes could be expressed separately in recombinant *Escherichia coli* and are both catalytically active. Biochemical analysis revealed that TTHB246 and TTHB247 have properties distinct from those of the BphI−BphJ complex. Chimeric complexes consisting of aldolase and dehydrogenase subunits from *T. thermophilus* and *B. xenovorans* were successfully constructed and characterized. This represents the first study of interspecies chimeric complexes derived from enzymes that exhibit substrate channeling.

EXPERIMENTAL PROCEDURES

Chemicals. Sodium pyruvate, acetaldehyde, propionaldehyde, coenzyme A, L-lactate dehydrogenase (LDH, rabbit muscle), alcohol dehydrogenase (*Saccharomyces cerevisiae*), and Chelex 100 were from Sigma-Aldrich (Oakville, ON). Aldehyde dehydrogenase was obtained from Calzyme (San Luis Obispo, CA). Restriction enzymes, T4 DNA ligase, and Pfx polymerase were from Invitrogen (Burlington, ON) or New England Biolabs (Pickering, ON). Ni-NTA Superflow resin was obtained from Qiagen (Mississauga, ON). All other chemicals were analytical grade and were obtained from Sigma-Aldrich and Fisher Scientific (Nepean, ON). 4-Hydroxy-2-oxopentanoate and 4-hydroxy-2-oxohexanoate were synthesized and purified as previously described.[11]

DNA Manipulation. DNA was purified, digested, and ligated using standard protocols.[18] The *bph*I and *bph*J genes were inserted into pBTL4-T7 and pET28a, respectively, as previously described[10] for coexpression with *T. thermophilus* enzymes. The gene encoding TTHB246 was amplified from genomic DNA, obtained from the RIKEN Bioresource Centre,[19] by polymerase chain reaction (PCR) using the primers GCGGCATATGAGCTGGGACCTTTCCACGG and GCACAAGCTTCTAGTCCGCGAGGGCCCC and the gene encoding TTHB247 with the primers GCGACATATGAGCGAAAGGGTTAAGGTAGCCATC and ATATTAAGCTTCACGCCACCACCTCCTCCACGG. Introduced *Nde*I and *Hin*dIII restriction sites are underlined. PCR mixtures contained 10 ng of genomic DNA, 0.1 unit of *Pfx* polymerase (Invitrogen), 20 nM amounts of each dNTP, 1× expand High Fidelity buffer, 1× *Pfx* enhancer, 1 mM $MgSO_4$, and each primer at 2 μM in a total volume of 50 μL. The following amplification profile was followed: 94 °C for 2 min, followed by 30 cycles of 94 °C for 30 s, 48 °C for 30 s, and 68 °C for 1 min and finally 68 °C for 10 min. The gene encoding TTHB247 was inserted into vector pET28a (EMD, Biosciences Inc., San Diego, CA), while the gene encoding TTHB246 was inserted into pBTL4-T7[10] for coexpression with BphJ or in pET28a for expression of the aldolase alone. Mutagenic primers for generating a TTHB246 A324G variant were as follows: CGGTGGGAGGGCAGGAGGACTGGATCCTG and CTGCCCTCCCACCGCCTGGCGGCGGCCG. Site-specific mutagenesis was performed according to a modified Quikchange (Stratagene) method that uses the partially overlapping primers mentioned above.[20] The following touchdown amplification profile was followed: 94 °C for 2 min, followed by eight cycles of 94 °C for 30 s, 60 °C for 1 min, and 72 °C for 6 min, followed by two successive runs of eight cycles with an annealing temperature of 55 and 50 °C. The PCR was completed with a final extension of 72 °C for 10 min. Genes from positive clones were sequenced at the Guelph Molecular Supercenter (University of Guelph) and were found to correspond to the genome sequence of *T. thermophilus* HB8 (GenBank entry AP008227).

Phylogenetic and Protein Interface Analysis. A multiple-sequence alignment containing orthologous aldolases and dehydrogenases was generated using ClustalX.[21] Amino acid conservation was mapped onto the structure of the DmpG−DmpF ortholog[22] using Consurf[23,24] and visualized using PyMOL.[25] Calculation of solvent accessible surfaces between interacting chains was completed using the crystal structure of the DmpG−DmpF complex[22] and the Protein Interfaces, Surfaces and Assemblies (PISA) server.[26] The evolutionary history was inferred by using the Maximum Likelihood method based on the JTT matrix-based model[27] from MEGA5.[28] Initial trees for the heuristic search were obtained automatically as follows. When the number of common sites was <100 or less than one-fourth of the total number of sites, the maximal parsimony method was used; otherwise, the BIONJ method with the MCL distance matrix was used. Trees were drawn to scale, with branch lengths measured in the number of substitutions per site. All positions containing gaps and missing data were eliminated.

Expression and Purification of Proteins. Recombinant *E. coli* BL21(λDE3) cells harboring the genes encoding TTHB246 or TTHB247 were propagated in 1 L of Luria-Bertani medium supplemented with 34 μg/mL kanamycin at 37 °C. When the optical density reached 0.6−0.8 at a wavelength of 600 nm, protein expression was induced by the addition of 1 mM IPTG to the culture. Following induction, cultures expressing the aldolase and dehydrogenase were incubated at 37 and 15 °C, respectively. Cells were harvested following overnight induction by centrifugation at 12096*g* for 10 min. Cells were lysed with a French press and centrifuged at 39191*g* for 25 min to remove cell debris. The supernatant was subjected to a 70 °C heat treatment for 10 min, followed by an additional centrifugation at 39191*g* for 25 min to remove precipitated proteins. The purification of each protein were performed by Ni^{2+}-NTA chromatography according to the protocol described for the BphI−BphJ complex.[10] The TTHB246−TTH247 complex was formed by incubation of 2 mg/mL TTHB246 and 2 mg/mL TTHB247 for 20 min at 25 °C. Complexes were concentrated and separated from uncomplexed protein using gel filtration on a HiLoad 26/60 Superdex 200 column at 25 °C in 20 mM HEPES buffer (pH 7.5) containing 150 mM NaCl, at a flow rate of 2 mL/min.

Chimeric aldolase−dehydrogenase complexes were expressed in *E. coli* BL21(λDE3) cells harboring the aldolase gene in vector pBTL4-T7 and the dehydrogenase gene in vector pET28a. Following Ni^{2+}-NTA chromatography,[10] the His tag was removed by thrombin cleavage and the proteins were subjected to gel filtration (HiLoad 26/60 Superdex 200). Purified enzymes were stored in 20 mM HEPES (pH 8.5) at −80 °C.

Determination of Protein Concentrations, Purities, and Molecular Masses. Protein concentrations were determined by the Bradford assay using bovine serum albumin as the standard.[29] Sodium dodecyl sulfate−polyacrylamide gel electrophoresis (SDS−PAGE) was performed, and the gels were stained with Coomassie Blue according to established procedures. The PageRuler Protein Ladder (Fermentas) containing proteins ranging from 10 to 220 kDa was used as molecular-mass markers.

The native molecular masses of purified aldolase, dehydrogenase, and the complex were estimated using gel filtration on a HiLoad 26/60 Superdex 200 column (GE Healthcare). Chromatography was conducted at 25 °C in 20 mM HEPES

buffer (pH 7.5) containing 150 mM NaCl, at a flow rate of 1 mL/min. Apparent molecular masses were calculated from the corresponding elution volumes using a calibration curve that was obtained with standard proteins.[10] The molecular masses of purified proteins were also determined by static light scattering using a Nano S Series Zetasizer (Malvern Instruments, Southborough, MA). Light scattering measurements were performed over five protein concentrations ranging from 0.5 to 5 mg/mL in triplicate at 25.0 ± 0.1 °C. The molecular mass was determined from a Debye plot using a specific refractive index increment of 0.185. Toluene (Sigma-Aldrich) and the buffer [20 mM HEPES (pH 8.5)] were used as references.

Divalent Metal Ion Specificity. Apo-aldolase enzymes were generated by incubation in 20 mM EDTA (pH 8.5) for 30 min at 25 °C followed by repeated dilution using metal free 20 mM HEPES buffer (pH 8.5) in a stirred cell containing a YM10 filter. The metal ion specificity of the aldolase was determined by incubating 10 μg of apo-aldolase with varying concentrations of metal chloride for 20 min followed by activity measurements using the standard aldol cleavage assays.[10,12] All buffers, reagents, and cofactors used in assays were prepared with highperformance liquid chromatography (HPLC) grade water and were additionally treated with Chelex 100 for 30 min to remove any remaining metal ion contaminants.

Aldolase Assays. Aldolase activity was deduced by assessing the production of pyruvate by coupling with NADH oxidation using LDH in a spectrophotometric assay. All assays were performed in at least duplicate in a total volume of 1 mL of 100 mM sodium HEPES buffer (pH 8.0) at 25 or 50 °C, using a Varian Cary 3 spectrophotometer equipped with a thermojacketed cuvette holder, and were initiated by adding 10 μg of enzyme, unless otherwise stated. The extinction coefficient of NADH at 340 nm was taken to be 6200 M^{-1} cm^{-1}. A standard aldolase activity assay contained 0.4 mM NADH, 1 mM $MnCl_2$ (for BphI) or 1 mM $CoCl_2$ (for TTHB246), and 19.2 units of LDH, and the level of the substrate was varied from 0.1K_m to 5K_m. The background rate was determined prior to addition of enzyme and subtracted from the results from the assays containing enzyme. One unit of enzyme represents the amount of protein that produces 1 μmol of pyruvate from substrate in 1 min. Data was fit by nonlinear regression to the Michaelis–Menten equation using Leonora.[30]

A discontinuous assay was performed in duplicate to determine the activity of the aldolase in complex with the dehydrogenase in the absence of cofactors. Assays contained 1 mM $MnCl_2$ or $CoCl_2$ and 20 μg of enzyme with the level of 4-hydroxy-2-oxopentanoate (HOPA) or 4-hydroxy-2-oxohexanoate (HOHA) varied from 0.1K_m to 5K_m in 100 mM HEPES buffer (pH 8.0). A solution without enzyme at each substrate concentration acted as a negative control. At 5 and 10 min intervals, reactions were quenched by addition of 20 mM EDTA (pH 8.5) and 0.4 mM NADH. The amount of pyruvate produced by the aldolase was determined by an end point assay by coupling to the stoichiometric oxidation of NADH by LDH.

Aldol addition assays with 2-ketobutyrate as the carbonyl donor were completed as previously described with 2-ketobutyrate concentrations ranging between 1 and 30 mM and the acetaldehyde concentration kept at 100 mM.[11,12]

Dehydrogenase Assays. Dehydrogenase assays were conducted using 0.4 mM NAD^+, 0.1 mM coenzyme A, and aldehyde concentrations that varied from at least 0.1K_m to 5K_m. All assays were performed in at least duplicate in a total volume of 1 mL of 100 mM sodium HEPES buffer (pH 8.0) at 25 °C, using a Varian Cary 3 spectrophotometer equipped with a thermojacketed cuvette holder, and were initiated by adding 2 μg of enzyme, unless otherwise stated. Concentrations of aldehyde stocks were determined by end point assays of NADH oxidation with alcohol dehydrogenase.

Thermostability Assays. Thermostability was tested at 50 °C in a digitally controlled water bath with an accuracy of ±0.1 °C using 1.5 mL microcentrifuge tubes containing 1 mg/mL enzyme in 20 mM HEPES buffer (pH 8.5). At given time points, an aliquot of the enzyme was removed and activity determined under standard conditions with 5K_m HOPA or acetaldehyde. Data were plotted using an exponential decay equation using SigmaPlot version 11.0.

Test of Substrate Channeling. The amount of aldehyde channeled directly from the aldolase to the dehydrogenase was assessed using an enzyme competition assay. All assays contained 100 μM HOPA or HOHA, 0.4 mM NAD^+, 0.1 mM coenzyme A, 1 mM $MnCl_2$, and 5 μg of enzyme complex with 20 units of aldehyde dehydrogenase (ALDH), which converts aldehydes to acids and reduces NAD^+. Reactions were completed in 100 mM HEPES buffer (pH 8.0) and were initiated via addition of substrate. The amount of NADH produced was measured spectrophotometrically and extrapolated to time zero. Reactions were quenched after 5 min with 24 μL of 3 N HCl, and mixtures were centrifuged for 3 min at 21000*g* to pellet the denatured enzyme. A 500 μL aliquot of the reaction mixture was subjected to HPLC using an ÄKTA Explorer 100 instrument (Amersham Pharmacia Biotech, Baie d'Urfe, QC) equipped with a HyPURITY C18 column (Thermo Scientific). The sample was eluted with 50 mM sodium phosphate (pH 5.3) and acetonitrile (47:3) for acetyl-CoA and propionyl-CoA. The channeling efficiency (eq 1) is calculated by comparing the acyl-CoA concentration (determined using HPLC) to the concentration of 4-hydroxy-2-oxoacid utilized by the aldolase based on the amount of NADH produced by the aldehyde dehydrogenases as previously described.[13]

$$\text{channeling efficiency (\%)} = \frac{[\text{acyl-CoA produced}]}{[\text{4-hydroxy-2-oxoacid utilized}]} \times 100\% \quad (1)$$

RESULTS

Phylogenetic Analysis of Aldolase and Dehydrogenase Homologues of BphI and BphJ. Amino acid sequences of aldolases and dehydrogenases from different bacteria were obtained from Uniprot[31] and separately aligned. Phylogenetic analysis revealed that the respective enzymes cluster similarly into six clades (Figure 1). The genes encoding enzymes within clades I–IV are within operons containing other aromatic *meta*-cleavage pathway genes that are arranged in a similar order in the genome of the respective organisms.[8,32−40] Members of these clades include DmpG and DmpF involved in phenol degradation in *P. putidia* CF600 (clade III) whose X- ray crystal structure is available and BphI and BphJ from the *B. xenovorans* PCB degradation pathway (clade IV) (Table S1 of the Supporting Information).[15,34,41] The enzymes from *T. thermophilus* (TTHB246 and TTHB247) appear to be evolutionarily divergent and form a separate group (clade V) in the phylogenetic tree (48 and 52% similar in sequence to BphI and BphJ, respectively). They are within operons that contain other genes encoding enzymes of the *meta*-cleavage pathway, but the order of these genes in the operon differs from those in clades I–IV. Members of clade VI on the other hand are unique in that they consist of members

dx.doi.org/10.1021/bi201832a | *Biochemistry* 2012, 51, 1942–1952

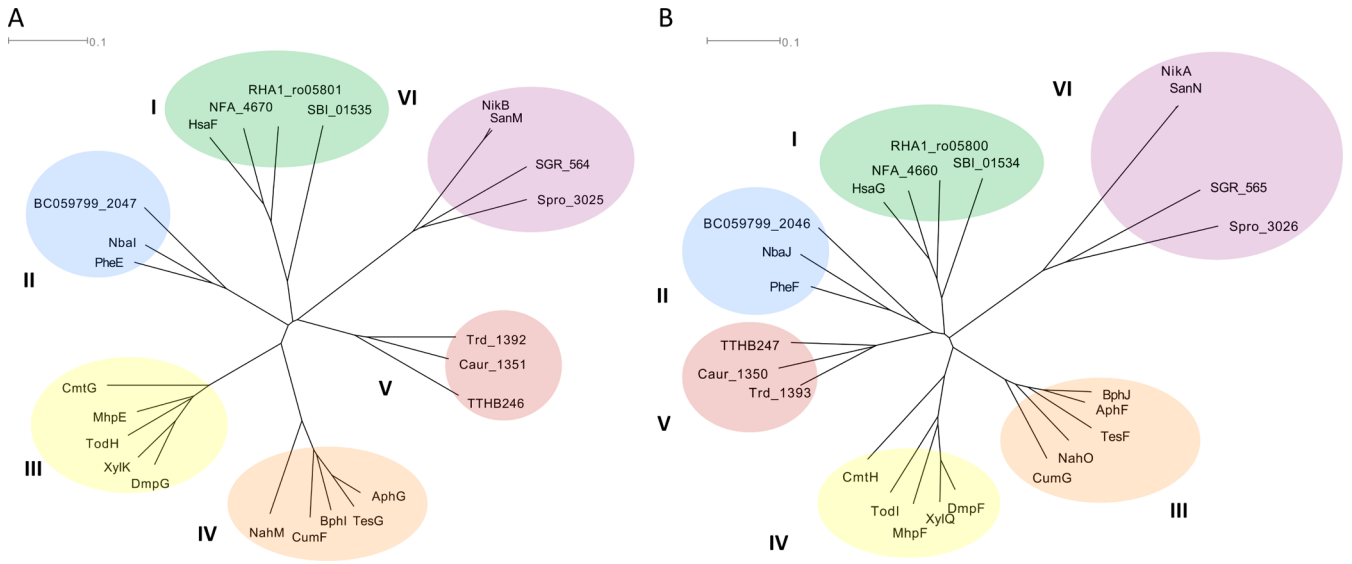

Figure 1. Dendrogram of the best trees obtained by alignment of 24 (A) aldolases and (B) dehydrogenases. The evolutionary history was inferred by using the maximum likelihood method based on the JTT matrix-based model.[27] The trees are drawn to scale, with branch lengths measured in the number of substitutions per site. All positions containing gaps and missing data were eliminated. The dendrogram was constructed using SplitsTree 4. Six distinct clades are present (I–VI); clades I–V contain enzymes involved in aromatic degradation pathways, and clade VI contains enzymes involved in biosynthetic pathways. Additional sequence information can be found in Table S1 of the Supporting Information.

(SanM and SanN, and NikB and NikA) that are part of a biosynthetic pathway of the antifungal nikkomycin.[16,17] The physiological reaction catalyzed by SanM and SanN and by NikB and NikA is the reverse of that of the homologous enzymes in the aromatic *meta*-cleavage pathways. In addition, these enzymes utilize 2-ketobutyrate as the carbonyl donor and picolinaldehyde as the electrophilic acceptor rather than pyruvate and aliphatic aldehydes, respectively. The other two members of clade VI (SGR_564 and Spro_3025) do not appear to be part of an antibiotic biosynthetic operon or an aromatic *meta*-cleavage pathway operon, and therefore, their physiological functions are not known.

Further analysis revealed that the dehydrogenase genes are encoded directly upstream of the aldolase genes in the genome of all representative members analyzed. The dehydrogenase genes from clades I–IV are preceded by a gene encoding a hydratase that catalyzes the step prior to the aldolase in the *meta*-cleavage pathway (Table S2 of the Supporting Information). Phylogenetic analysis of these hydratases revealed that some members (DmpE, XylJ, and NahL) are not clustered in the clades as the corresponding aldolases and dehydrogenases from the same organisms (Figure S1 of the Supporting Information).

Expression and Purification of *T. thermophilus* Enzymes and Chimeric *T. thermophilus*–*B. xenovorans* Enzyme Complexes. The *T. thermophilus* enzymes were separately expressed in soluble form and purified to homogeneity using Ni^{2+}-NTA chromatography. Typical yields of each protein were 20 mg of purified protein per liter of bacterial culture. The molecular masses of TTHB246 and TTHB247 as estimated by SDS–PAGE were 37 and 33 kDa, respectively (Figure 2A,B), which are in agreement with the predicted molecular masses calculated from their respective amino acid sequences. The native molecular masses of TTHB246 and TTHB247, determined by gel filtration and static light scattering, correspond to a dimer for the aldolase and a monomer for the dehydrogenase, respectively (Table 1). On the other hand, the native molecular mass of the protein mixture containing TTHB246 and TTHB247 (Figure 3A and Table 1) was consistent with a

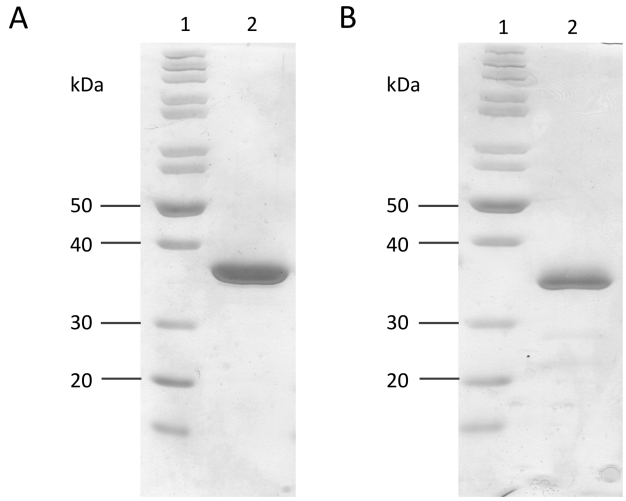

Figure 2. Coomassie Blue-stained SDS–polyacrylamide gel of purified TTHB246 and TTHB247. Gel loaded with (A) TTHB246 and (B) TTHB247 following purification using Ni^{2+}-NTA and cleavage of the histidine tag (lane 2). The molecular masses of the proteins in the standard (lane 1) are indicated beside the gel. The molecular masses of TTHB246 and TTHB247 as determined from the gel are 37 and 33 kDa, respectively.

heterotetramer with two aldolase and two dehydrogenase subunits per complex, similar to the oligomeric state observed in the crystal structure of the DmpG–DmpF complex (Figure 4A).[22]

Chimeric complexes of the *B. xenovorans* and *T. thermophilus* enzymes (TTHB246–BphJ and BphI–TTHB247) were created by coexpression of the relevant genes in *E. coli* using separate expression plasmids. Although only the dehydrogenase encodes a histidine tag, association of the aldolase with the dehydrogenase in these chimeric complexes was sufficiently tight to allow for the copurification of the aldolase by Ni^{2+}-NTA chromatography (Figure 3B). Subsequent analysis by gel filtration and static light scattering of purified proteins (Table 1)

dx.doi.org/10.1021/bi201832a | *Biochemistry* 2012, 51, 1942–1952

Table 1. Determination of Oligomeric Molecular Masses Using Size Exclusion Chromatography and Static Light Scattering[a]

protein	molecular mass determined by size exclusion chromatography (kDa)	molecular mass determined by static light scattering (kDa)
TTHB246	72 ± 8	78 ± 4
TTHB247	40 ± 5	33 ± 1
TTHB246–TTHB247	142 ± 18	152 ± 10
BphI–TTHB247	144 ± 18	137 ± 12
TTHB246–BphJ	144 ± 18	145 ± 13

[a]Theroretical molecular masses as calculated by amino acid sequences are 36.8 kDa for BphI, 32.2 kDa for BphJ, 37.2 kDa for TTHB246, and 33.1 kDa for TTHB247.

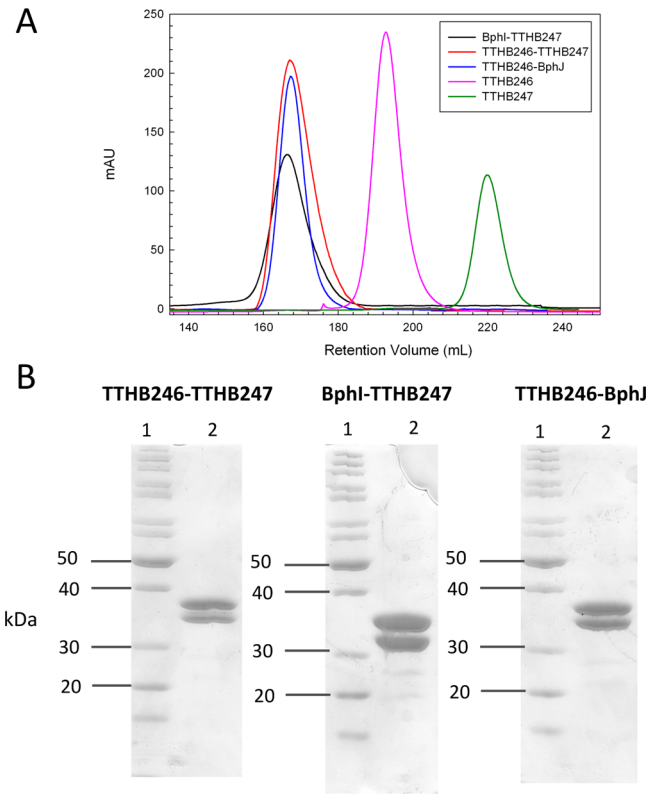

Figure 3. Determination of molecular masses of proteins by exclusion column chromatography and SDS–PAGE. (A) FPLC traces of elution profiles detected at 280 nm. Three distinct peaks can be resolved corresponding to the sizes of a tetramer for the TTHB246–TTHB247 complex, a dimer for TTHB246, and a monomer for TTHB247. (B) Coomassie Blue-stained SDS–polyacrylamide gels of purified aldolase–dehydrogenase complexes after elution from gel filtration and concentration using a YM10 filter. The molecular masses of the proteins in the standard are indicated.

suggested that the chimeras have a tetrameric quaternary structure similar to that of their native complexes.

Metal Cofactor Specificity of TTHB246. Kinetic parameters of TTHB246 with a variety of divalent metal ions were determined (Table 2). The apoenzyme had <0.5% activity relative to that of the enzyme incubated with 1 mM Co^{2+}. TTHB246 had the highest specificity for Co^{2+} followed by Ni^{2+} and Mn^{2+}. This differs from BphI, in which Mn^{2+} was found to give the highest activity while the Co^{2+} enzyme exhibited a 5-fold lower activity than the Mn^{2+}-containing

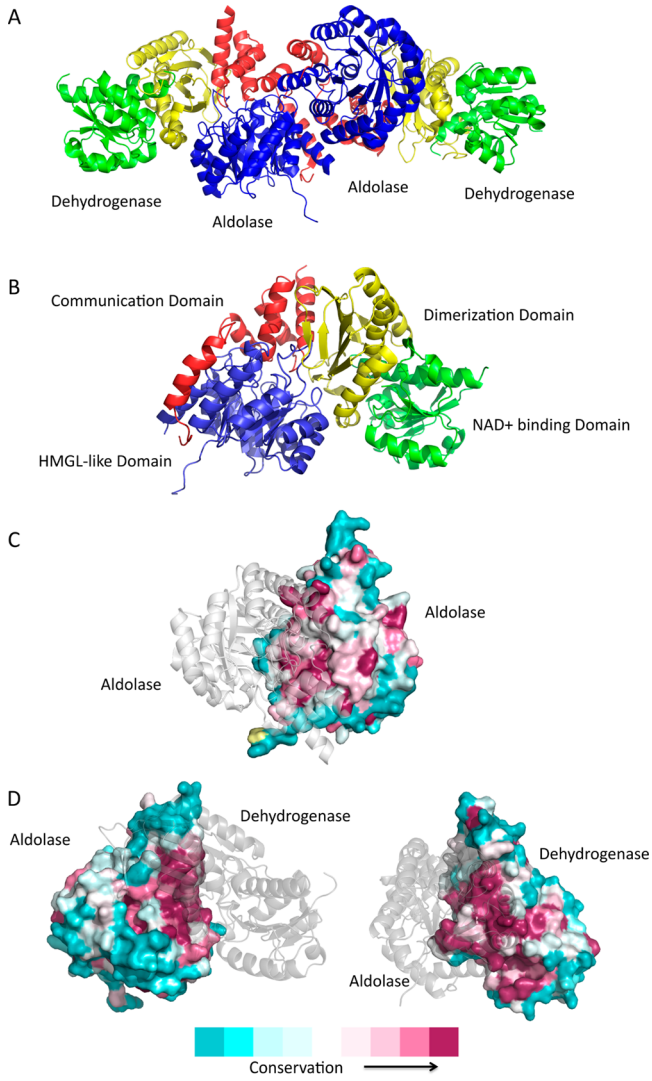

Figure 4. Structure of the aldolase–dehydrogenase complex showing the domains in each enzyme and conservation of residues in the enzymes. (A) Cartoon representation of the hetereotetrameric configuration of the DmpG–DmpF complex as observed in the crystal structure. (B) Cartoon representation of an aldolase–dehydrogenase dimer showing four distinct domains. The HMGL-like domain (residues 1–250), colored blue, is located on the N-terminus of the aldolase, while a five-α-helix communication domain (residues 251–345), colored red, composes the C-terminal end of the protein. Both domains contribute residues that interact with the dehydrogenase. The dehydrogenase is composed of a Rossmann fold N-terminal NAD^+-binding domain (residues 1–130 and 286–312, colored green) and a C-terminal dimerization domain (residues 131–285, colored yellow) and exclusively forms protein–protein interactions with the aldolase. (C) Conservation of residues in orthologous aldolases at the aldolase–aldolase interface. The crystal structure of the DmpG–DmpF complex was used as a template, and conserved residues in the aldolases were mapped to this structure using the previously generated sequence alignment. One aldolase subunit in the dimer is represented as a space-filled model and colored according to the conservation scores, while the other is depicted as a gray cartoon. Highly conserved residues are colored red, while highly variable residues are colored teal; the intensity is directly proportional to the degree of conservation. (D) Conserved residues in orthologous aldolase–dehydrogenase complexes at the aldolase–dehydrogenase interface. The aldolase (left) and dehydrogenase (right) are represented as space-filled models and colored according to the conservation scores as before. The structures of partner enzymes are depicted as gray cartoons. Phylogenetic mapping was completed using the Consurf server,[23,24] and structures were visualized using PyMOL.[25]

dx.doi.org/10.1021/bi201832a | *Biochemistry* 2012, 51, 1942–1952

Table 2. Relative Activities of TTHB246 with Various Divalent Metal Ions[a]

metal ion	$K_{m,app}$ (μM)	k_{cat} (s^{-1})	$k_{cat}/K_{m,app}$ ($\times 10^4$ $M^{-1}s^{-1}$)	relative k_{cat} (%)
Co^{2+}	55 ± 4	1.0 ± 0.02	1.9 ± 0.13	100 ± 2.6
Ni^{2+}	74 ± 6	0.79 ± 0.03	1.1 ± 0.10	75.4 ± 2.8
Mn^{2+}	45 ± 6	0.57 ± 0.03	1.3 ± 0.20	57.0 ± 2.1
Mg^{2+}	80 ± 7	0.13 ± 0.03	0.16 ± 0.04	12.5 ± 3.2
Ca^{2+}	95 ± 9	0.08 ± 0.001	0.08 ± 0.008	8.2 ± 2.8

[a]The activity obtained with $CoCl_2$ is taken to be 100%. Assays were performed with 30 μg of enzyme, 2 mM 4-hydroxy-2-oxopentanoate, 0.4 mM NADH, 19.2 units of LDH, and metal chloride salts with concentrations varying between at least 0.1K_m and 10K_m, in 100 mM HEPES buffer (pH 8.0) at 25 °C in a total volume of 1 mL.

enzyme.[10] Cd^{2+}- and Cu^{2+}-containing enzymes exhibited no detectable aldol cleavage activity (<0.0001 s^{-1}).

Thermostability. TTHB247 had a half-life of only 1.6 h at 50 °C. The half-life of TTHB246 at the same temperature was ~40 h longer. Interestingly, when these enzymes are in complex, the half-life of TTHB246 was reduced by approximately 30 h while that of TTHB247 was increased by ~4 h relative to that of the uncomplexed enzyme (Table 3). In comparison, the

Table 3. Half-Lives of Aldolases and Dehydrogenases at 50 °C[a]

enzyme	half-life (h)	
	aldol cleavage activity	dehydrogenase activity
TTHB246	42 ± 5	–
TTHB247	–	1.64 ± 0.05
TTHB246–TTHB247	10.0 ± 0.7	5.9 ± 0.5
BphI–BphJ	0.220 ± 0.002	0.21 ± 0.01
TTHB246–BphJ	2.66 ± 0.2	1.62 ± 0.1
BphI–TTHB247	0.54 ± 0.03	2.47 ± 0.2

[a]Thermostability was determined at 50 °C in a digitally controlled water bath with an accuracy of ±0.1 °C using 1.5 mL microcentrifuge tubes containing a 1 mg/mL enzyme solution in 20 mM HEPES buffer (pH 8.5). At given time points, an aliquot of the enzyme was removed and assayed under standard conditions with a saturating level of substrate, yielding the steady state kinetic activity.

BphI–BphJ complex was found to be very unstable at 50 °C, with both enzymes exhibiting a half-life of approximately 13 min. Partnered with a thermostable counterpart in the chimeric complex, the Bph enzymes were more stable than in their native complex. TTHB246 exhibited lower stability in these chimeric complexes, whereas the stability of both enzymes in the BphI–TTHB247 complex improved compared to that of BphI in its native complex and uncomplexed TTHB247.

Steady State Kinetic Analysis. Similar to BphI, TTHB246 exhibited stereochemical control as the aldolase was able to catalyze the cleavage of only one enantiomer of HOPA [(4*S*)-HOPA] and HOHA.[11,42] TTHB246 exhibited similar catalytic parameters for these two substrates (Table 4). TTHB246 was not able to catalyze the aldol addition of 2-ketobutyrate with acetaldehyde. This indicates that like BphI,[11,12] the enzyme is specific for pyruvate as the carbonyl donor. TTHB247 exhibited similar kinetic parameters for acetaldehyde and propionaldehyde. However, in both circumstances, the catalytic parameters were dependent on the oligomeric state of the enzyme (Table 5). For instance, the catalytic efficiency (k_{cat}/K_m) of TTHB246 for both 4-hydroxy-2-oxoacids was increased (~3-fold) when it was in complex with TTHB247, primarily because of decreases in K_m values. Conversely, k_{cat}/K_m for aldehydes decreased ~3-fold in the TTHB246–TTHB247 complex compared to that of uncomplexed TTHB247, because of increases in K_m values. Using HOPA as a substrate, kinetic parameters were also determined at 50 °C for TTHB246 alone and TTHB246 in complex with TTHB247. While the K_m value was not affected by the increase in temperature, the k_{cat} value increased marginally by approximately 4-fold. Because of the volatility of aldehydes, dehydrogenase assays could not be reliably performed at 50 °C.

In the TTHB246–BphJ and BphI–TTHB247 chimeric complexes, K_m values for HOPA in the aldolases were 3–5-fold higher than those of their native heterotetrameric complexes. The k_{cat} value for TTHB246 in complex with BphJ increased 4-fold compared to k_{cat} of its native complex, while that of the BphI in complex with TTHB247 decreased 2-fold. A similar trend was observed for the aldolase kinetic parameters in the chimeras for the substrate HOHA. The most significant change in kinetic parameters was observed in the TTHB246–BphJ complex, where the k_{cat} for BphJ was reduced ~5-fold for acetaldehyde and propionaldehyde in comparison to that of the native BphI–BphJ complex.

Substrate Channeling and Activation. It was previously determined that the BphI–BphJ complex channels acetaldehyde and propionaldehyde with 95 ± 5% efficiency.[13] Using the same assay, the TTHB246–TTHB247 complex was observed to channel acetaldehyde, the intermediate produced from the cleavage of HOPA, with an efficiency similar to that of the BphI–BphJ complex (94 ± 1%). However, the channeling efficiency for propionaldehyde was ~57% (Table 6). The replacement of an alanine residue (A324) that is proposed, on the basis of the work with the BphI–BphJ complex,[13] to line the aldehyde channel in the aldolase with glycine resulted in a channeling efficiency of 94 ± 1% for propionaldehyde. Chimeric complexes, on the other hand, were observed to exhibit a low but detectable substrate channeling efficiency of ~10% for acetaldehyde.

In the presence of the NADH cofactor, TTHB246 exhibited a 2-fold increase in k_{cat}. This is slightly lower than that of the BphI–BphJ complex, where 5-fold activation was reported.[13] Neither chimeric complex was activated by the presence of the nicotinamide cofactor (Table 7). When the aldolase and dehydrogenase reactions were coupled, the k_{cat} of the overall reaction with HOPA as the substrate in the TTHB246–BphJ chimeric complex did not exceed the k_{cat} of TTHB246 alone, indicating that TTHB246 activity is not increased when BphJ is undergoing turnover.

Analysis of Interacting Residues in the Aldolase–Dehydrogenase Complex. Residues interacting between enzyme subunits were analyzed on the basis of the available crystal structure of the DmpG–DmpF complex (PDB entry 1NVM),[22] which is orthologous to the BphI–BphJ and TTHB246–TTHB247 complexes. The aldolase is comprised of two domains: an N-terminal HMGL-like TIM barrel domain that is composed of residues 19–251 and a C-terminal α-helical domain, termed a communication domain, of residues 275–340.[22] The dehydrogenase is also composed of two domains: an N-terminal NAD^+ binding domain fold spanning residues 6–119 and a C-terminal dimerization domain of residues 127–273 (Figure 4B). The average dimer interface area between adjacent aldolases is 1499.6 $Å^2$, with a Δ^iG of −15.8 kcal/mol (p = 0.044) (Figure 4C).

dx.doi.org/10.1021/bi201832a | *Biochemistry* 2012, 51, 1942–1952

Table 4. Steady State Kinetic Parameters of Aldolases TTHB246 and BphI[a]

		HOPA			HOHA		
aldolase	dehydrogenase	K_m (μM)	k_{cat} (s^{-1})	k_{cat}/K_m ($\times 10^4$ M^{-1} s^{-1})	K_m (μM)	k_{cat} (s^{-1})	k_{cat}/K_m ($\times 10^4$ M^{-1} s^{-1})
TTHB246		206 ± 17	1.0 ± 0.03	5.0 ± 0.5	210 ± 15	1.1 ± 0.03	5.2 ± 0.5
TTHB246	TTHB247	41 ± 3	0.6 ± 0.01	14.0 ± 0.01	37 ± 3	0.5 ± 0.01	13 ± 0.01
TTHB246	BphJ	257 ± 11	2.4 ± 0.04	9.4 ± 0.4	218 ± 11	2.2 ± 0.04	10 ± 0.05
BphI	TTHB247	295 ± 20	2.3 ± 0.03	7.8 ± 0.5	199 ± 10	2.1 ± 0.03	11 ± 0.05
BphI	BphJ	89 ± 8	4.1 ± 0.1	46 ± 4	117 ± 10	3.9 ± 0.2	33 ± 2

[a]Assays were performed at 25 °C and contained 0.4 mM NADH, 1 mM $MnCl_2$ (for BphI) or $CoCl_2$ (for TTHB246), and 19.2 units of LDH in 100 mM HEPES buffer (pH 8.0) in a total volume of 1 mL.

Table 5. Steady State Kinetic Parameters of Dehydrogenases TTHB247 and BphJ toward Acetaldehyde and Propionaldehyde[a]

		acetaldehyde			propionaldehyde		
dehydrogenase	aldolase	$K_{m,app}$ (mM)	k_{cat} (s^{-1})	$k_{cat}/K_{m,app}$ ($\times 10^2$ M^{-1} s^{-1})	$K_{m,app}$ (mM)	k_{cat} (s^{-1})	$k_{cat}/K_{m,app}$ ($\times 10^2$ M^{-1} s^{-1})
TTHB247	–	5.5 ± 0.5	7.4 ± 0.04	13.5 ± 1.2	6.4 ± 0.6	8.4 ± 0.04	13.1 ± 1.2
TTHB247	TTHB246	15.4 ± 1.5	3.5 ± 0.01	2.3 ± 0.3	16.1 ± 1.3	3.6 ± 0.02	2.2 ± 0.03
TTHB247	BphI	9.4 ± 0.8	2.8 ± 0.07	3.0 ± 0.3	9.6 ± 0.8	2.6 ± 0.07	2.7 ± 0.2
BphJ	TTHB246	15.7 ± 1.3	2.2 ± 0.06	1.4 ± 0.1	16.1 ± 1.2	2.3 ± 0.05	1.4 ± 0.1
BphJ	BphI	23.6 ± 1.8	17.2 ± 0.5	7.3 ± 0.06	23.1 ± 1.7	16.3 ± 0.5	7.0 ± 0.05

[a]Assays were performed at 25 °C and contained 0.4 mM NAD^+ and 0.1 mM coenzyme A in 100 mM HEPES buffer (pH 8.0) in a total volume of 1 mL.

Table 6. Substrate Channeling Efficiencies in Enzyme Complexes[a]

		channeling efficiency (%)	
enzyme	substrate	acetaldehyde	propionaldehyde
TTHB246	TTHB247	94 ± 1	57 ± 2
BphI	TTHB247	9 ± 2	–
TTHB246	BphJ	12 ± 1	–
TTHB246	TTHB247 (A324G)	94 ± 4	94 ± 1

[a]Assays were performed at 25 °C and contained 0.4 mM NAD^+, 0.1 mM coenzyme A, 1 mM $MnCl_2$, and 10 μg of enzyme in the presence of excess ALDH. The substrate concentration was 100 μM (*S*)-HOPA or HOHA. NADH production was measured spectrophotometrically at 340 nm, and CoA esters were detected at 254 nm using HPLC.

The dimer interface is primarily composed of highly conserved hydrophobic residues. The interface between the aldolase and dehydrogenase, on the other hand, has an average area of 1458.2 Å^2, with a Δ^iG of only −9.9 kcal/mol (p = 0.244). Forty-two amino acid residues of each enzyme contribute to the aldolase−dehydrogenase interface (Figure 4D). In the aldolase, the TIM barrel domain contributes 27 of the 42 residues, with the remainder contributed by the extreme C-terminus of the α-helical communication domain. On the other hand, the C-terminal dimerization domain of the dehydrogenase contributes all 42 interacting residues. While hydrophobic residues predominantly constitute the amino acids at the interface between aldolase and dehydrogenase, four salt bridges are present in the crystal structure of the DmpG−DmpF complex (Figure 5A). The residues that form salt bridges are largely conserved among homologues with the exception of the TTHB246−TTHB247 complex, where Lys-304 and Asp-331 in DmpG are replaced with glutamate and arginine, respectively, in TTHB246 and their paired residues, Asp-250 and Arg-208 in DmpF, are replaced with glutamate and threonine, respectively, in TTHB247 (Figure 5B). These substitutions have the potential for charge repulsion in the TTHB246−BphJ chimera because of the proximity of Arg-207 with Arg-330 and Arg-66 with Arg-176. No obvious charge repulsions between interacting side chains were identified in the BphI−TTHB246 chimera.

In DmpF, amino acids 250−268 form a loop containing an antiparallel β-sheet. This loop, which is unique to clade III, is responsible for the formation of a hydrophobic interaction with the aldolase as Leu-258 and Ile-260 in the middle of the loop interact with Phe-64 of the aldolase while Pro-261 interacts with Gly-65 and the β-methyl of Thr-68 of the aldolase. Clade V dehydrogenases, including TTHB247, contain a shorter loop, while clade IV dehydrogenases, including BphJ, do not contain this motif. However, there are no significant alterations in the amino acid residues at the interface in the corresponding aldolases of clade II in comparison to those in clades I and III.

DISCUSSION

Phylogenetic analysis revealed that the aldolases and dehydrogenases homologous to BphI and BphJ are clustered similarly into six clades based on amino acid sequence similarities. The enzymes TTHB246 and TTHB247 from *T. thermophilus* HB8 belong to a clade distinct from that of the well-characterized orthologs, BphI and BphJ from *B. xenoverans* LB400, and biochemical characterization revealed that their properties are distinct from those of the Bph enzymes.

The TTHB246−TTHB247 complex was able to channel acetaldehyde efficiently (>90%), but a channeling efficiency of only ∼57% was observed for the larger propionaldehyde. Significantly, a residue corresponding to Gly-322 of BphI is an alanine in TTHB246. Gly-322 is located at the narrowest diameter of the channel of BphI that links the aldolase and the dehydrogenase active sites, and previous substitution of Gly-322 with the larger alanine in BphI by site-specific mutagenesis led to a reduction in the channeling efficiency for propionaldehyde in BphI−BphJ complex of ∼40%.[13] This substitution effectively causes a partial steric blockage in the channel manifested by a decreased channeling efficiency for propionaldehyde but not the smaller acetaldehyde. A single A324G substitution in TTHB246 was able to increase propionaldehyde channeling efficiency to that observed for acetaldehyde.

Table 7. Kinetic Parameters of the Aldol Cleavage Reaction of 4-Hydroxy-2-oxopentanoate in the Absence of NADH[a]

enzyme	substrate	$K_{m,app}$ (μM)	k_{cat} (s^{-1})	$k_{cat}/K_{m,app}$ ($\times 10^3$ M^{-1} s^{-1})	x-fold activation by NADH
BphI	BphJ	158 ± 20	0.8 ± 0.06	5.1 ± 0.4	5.1 ± 0.4
TTHB246	TTHB247	123 ± 15	0.3 ± 0.01	2.9 ± 0.1	2.0 ± 0.07
TTHB246	BphJ	253 ± 19	2.4 ± 0.06	9.3 ± 0.8	1.0 ± 0.03
BphI	TTHB247	290 ± 27	2.3 ± 0.07	7.9 ± 0.3	1.0 ± 0.03

[a]Assays were completed in a discontinuous fashion and contained 1 mM $MnCl_2$ or 1 mM $CoCl_2$. HOPA concentrations varied from 0.1K_m to 10K_m in 100 mM HEPES buffer (pH 8.0). At 10 min, the reaction was quenched with 20 mM EDTA and 0.1 mM NADH. The amount of pyruvate produced by the aldolase was determined by an end point assay by coupling to the stoichiometric oxidation of NADH by LDH.

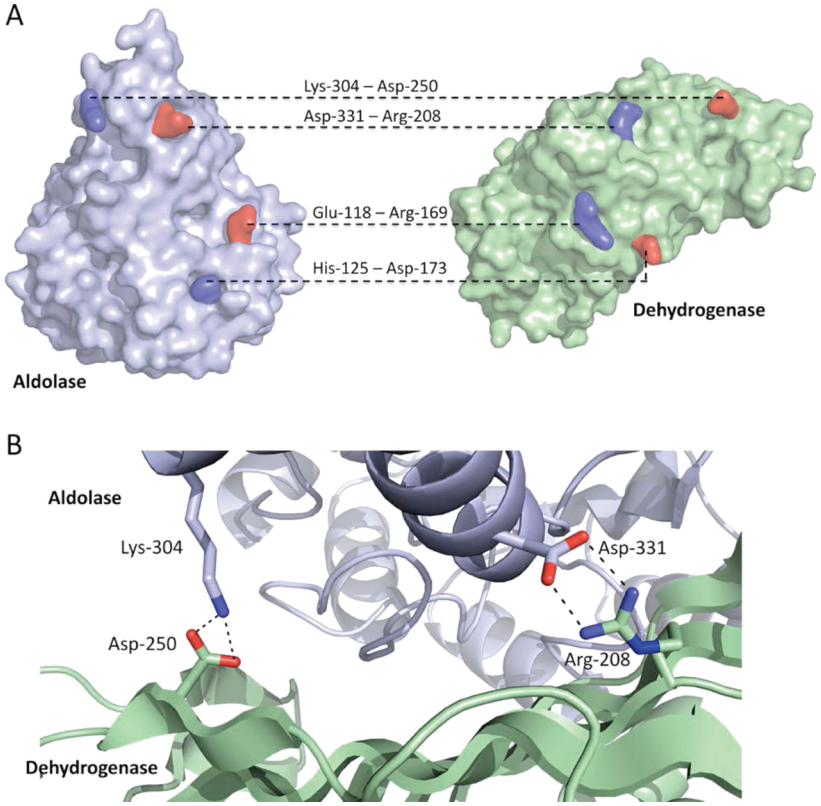

Figure 5. Salt bridges found in the aldolase–dehydrogenase interface. (A) Salt bridges in the DmpG–DmpF complex are shown; red and blue residues represent the respective charges of the amino acid side chains. The aldolase (blue) and dehydrogenase (green) are represented as space-filled models. (B) Identification of salt bridges that are not conserved in the TTHB246–TTHB247 complex. The enzymes are depicted as a cartoon, while identified residues are shown as sticks with carbon atoms colored according to their respective enzyme colors. Salt bridges were identified using the Protein Interfaces, Surfaces and Assemblies (PISA) server[26] and visualized using PyMOL.[25]

All aldolases that group with TTHB246 (clade V) as well as aldolases in clade VI in the phylogenetic tree have alanine residues that correspond to Gly-322 of BphI. Group VI members include SanM and NikA, which utilize bulky picolinaldehyde as a substrate, and the potential constriction in the channel suggests that this aldehyde may diffuse through the bulk solvent from one enzyme to another rather than through the molecular channel. Because all other amino acid residues proposed to compose the channel are conserved across homologues, the channel dimensions and locations in these enzymes are likely to be similar to that reported for the BphI–BphJ complex.[13]

Unlike other aldolase–dehydrogenase complexes, TTHB246 and TTHB247 can be separately expressed in recombinant *E. coli* and are both catalytically active.[10,14,17] This contrasts with the reported inactivity of the aldolase from the nikkomycin biosynthetic pathway, SanM, when it is not in complex with the corresponding dehydrogenase, SanN.[17] In comparison, the α and β subunits of tryptophan synthase, another enzyme system that exhibits substrate channeling,[43] are catalytically active when purified individually, but their activities are 1–2 orders of magnitude higher when they are in complex.[44]

Analysis by gel filtration and static light scattering indicated that the oligomeric state of the aldolase TTHB246 is a dimer, while the oligomeric state of the dehydrogenase is a monomer. However, these enzymes had the propensity to form a stable heterotetramer in vitro when both proteins were present. This indicates that formation of the tetrameric complex occurs via the association of the dehydrogenase to the aldolase dimer and not the association of two heterodimers. Once formed, the tetrameric complex was stable and did not dissociate into smaller oligomeric units. Similarly, it has been reported that the DmpG–DmpF heterotetramer cannot be separated using various chromatography methods in both high- and low-ionic strength solutions.[34]

Interestingly, upon formation of the complex, the catalytic efficiency of the aldolase was increased while that of the dehydrogenase was decreased relative to those of the free enzymes. In the

dx.doi.org/10.1021/bi201832a | *Biochemistry* 2012, 51, 1942–1952

complexed state, the K_m value for TTHB246 was reduced 4-fold while that of TTHB247 was increased 3-fold relative to those of the unassociated enzymes. The k_{cat} value, on the other hand, was reduced by ~2-fold in the complexed enzymes relative to the uncomplexed enzymes. However, the thermal stability of the TTHB247 was enhanced in the complex, while TTHB246 was less thermostable when in complex with TTHB247. In contrast, it has been reported that formation of the $\alpha\beta\beta\alpha$ complex in tryptophan synthase from *Thermotoga maritima* resulted in a 1−3-fold increase in the half-life at 85 °C, and in this case, both the α and β subunits had improved thermostability upon formation of the complex.[45] Formation of the complex between TTHB246 and TTHB247 is nevertheless beneficial because of the increased catalytic efficiency as a result of substrate channeling.

As expected from the high degree of conservation of residues at the interface between aldolase and dehydrogenase subunits, chimeric complexes of *T. thermophilus* and *B. xenovorans* are stable and could be copurified by gel filtration and affinity chromatography. While aldehyde channeling occurs, the efficiencies of acetaldehyde channeling in these chimeric complexes are low. Detailed analysis using multiple-sequence alignments and the crystal structure of the DmpG−DmpF complex revealed potential charge−charge repulsion in the TTHB246−BphJ chimera that may prevent proper alignment of enzyme subunits. Thus, the low channeling efficiency observed in this chimeric complex may be the result of aldehydes escaping from the subunit interface. No obvious unfavorable side chain interactions can be seen in the BphI−TTHB247 complex. Alternatively, improper coupling and communication between enzyme subunits could also result in a reduced efficiency of substrate channeling.

Previous studies with tryptophan synthase suggest that coevolution of enzymes within an enzyme complex may be required to establish stable interactions that are prerequisites for efficient substrate channeling.[46] The genes encoding the aldolase and dehydrogenase that we analyzed in this study are adjacent in the genomes of different bacteria, and linkage analysis based on the encoded amino acid sequences showed that they cluster similarly in their phylogenetic trees. However, differences in the phylogenetic tree of corresponding hydratases encoded within the same operon indicate that the similar phylogenetic clustering of aldolases and dehydrogenases cannot be entirely ascribed to random sequence drift of genes in different bacterial species.[47] Similarity in the phylogenetic tree of interacting proteins has also been observed in other systems, such as insulin and insulin receptors,[48] dockerins and cohexins,[49] and vasopressins and vasopressin receptors.[50]

In summary, TTHB246 and TTHB247 exhibit unique biophysical properties that allow them to be individually expressed while maintaining catalytic activity. The complex is different from the BphI−BphJ complex in that it preferentially channels acetaldehyde over propionaldehyde and appears to be allosterically activated to a lesser degree. However, phylogenetic analysis revealed that residues involved in protein−protein interactions in the TTHB246−TTH247 complex and orthologous complexes are highly conserved, allowing for the association of enzymes from different bacterial species as demonstrated by the successful construction of chimeric complexes. However, fine-tuning of this interaction appears to be important for ensuring efficient substrate channeling between the aldolase and dehydrogenase. Finally, it should be noted that because the aldolase exhibits identical stereochemical control and amino acid residues that compose the active site of TTHB246 are conserved in BphI, previous modifications to BphI could be applied to TTHB246 to create a more stable enzyme that is suitable for industrial synthesis of chiral 4-hydroxy-2-oxoacid skeletons as synthons for organic reactions.[42]

■ ASSOCIATED CONTENT

Supporting Information

Dendrogram of alignment of hydratases encoded on operons that precede dehydrogenases (Figure S1), phylogenetic information for homologues of TTHB246 and TTHB247 (Table S1), comparison of sequence identity between homologous aldolases (Table S2), comparison of sequence identity between homologous dehydrogenases (Table S3), and information about hydratases used in the phylogenetic tree (Table S4). This material is available free of charge via the Internet at http://pubs.acs.org.

■ AUTHOR INFORMATION

Corresponding Author

*Department of Molecular and Cellular Biology University of Guelph, Guelph, Ontario, Canada N1G 2W1. E-mail: sseah@uoguelph.ca. Phone: (519) 824-4120, ext. 56750. Fax: (519) 837-1802.

Funding

This research is supported by the National Science and Engineering Research Council of Canada (NSERC), Grant 238284 (to S.Y.K.S.). P.B. and C.H. are recipients of an NSERC PGS-D scholarship and USRA studentship, respectively.

Notes

The authors declare no competing financial interest.

■ ABBREVIATIONS

ALDH, aldehyde dehydrogenase; HEPES, 4-(2-hydroxyethyl)-1-piperazineethanesulfonic acid; HOHA, 4-hydroxy-2-oxohexanoate; HOPA, 4-hydroxy-2-oxopentanoate; IPTG, isopropyl β-D-thiogalactopyranoside; LDH, L-lactate dehydrogenase.

■ REFERENCES

(1) Phizicky, E. M., and Fields, S. (1995) Protein-protein interactions: Methods for detection and analysis. *Microbiol. Rev. 59*, 94−123.

(2) Hawkins, A. R., and Lamb, H. K. (1995) The molecular biology of multidomain proteins. Selected examples. *Eur. J. Biochem. 232*, 7−18.

(3) Khan, S. H., Ahmad, F., Ahmad, N., Flynn, D. C., and Kumar, R. (2011) Protein-protein interactions: Principles, techniques, and their potential role in new drug development. *J. Biomol. Struct. Dyn. 28*, 929−938.

(4) Nagradova, N. K. (2001) Interdomain interactions in oligomeric enzymes: Creation of asymmetry in homo-oligomers and role in metabolite channeling between active centers of hetero-oligomers. *FEBS Lett. 487*, 327−332.

(5) Miles, E. W., Rhee, S., and Davies, D. R. (1999) The molecular basis of substrate channeling. *J. Biol. Chem. 274*, 12193−12196.

(6) Huang, X., Holden, H. M., and Raushel, F. M. (2001) Channeling of substrates and intermediates in enzyme-catalyzed reactions. *Annu. Rev. Biochem. 70*, 149−180.

(7) Raushel, F. M., Thoden, J. B., and Holden, H. M. (2003) Enzymes with molecular tunnels. *Acc. Chem. Res. 36*, 539−548.

(8) Hofer, B., Backhaus, S., and Timmis, K. N. (1994) The biphenyl/polychlorinated biphenyl-degradation locus (bph) of *Pseudomonas* sp. LB400 encodes four additional metabolic enzymes. *Gene 144*, 9−16.

(9) Denef, V. J., Park, J., Tsoi, T. V., Rouillard, J. M., Zhang, H., Wibbenmeyer, J. A., Verstraete, W., Gulari, E., Hashsham, S. A., and Tiedje, J. M. (2004) Biphenyl and benzoate metabolism in a genomic context: Outlining genome-wide metabolic networks in *Burkholderia xenovorans* LB400. *Appl. Environ. Microbiol. 70*, 4961−4970.
(10) Baker, P., Pan, D., Carere, J., Rossi, A., Wang, W., and Seah, S. Y. (2009) Characterization of an aldolase-dehydrogenase complex that exhibits substrate channeling in the polychlorinated biphenyls degradation pathway. *Biochemistry 48*, 6551−6558.
(11) Wang, W., Baker, P., and Seah, S. Y. (2010) Comparison of two metal-dependent pyruvate aldolases related by convergent evolution: Substrate specificity, kinetic mechanism, and substrate channeling. *Biochemistry 49*, 3774−3782.
(12) Baker, P., Carere, J., and Seah, S. Y. (2011) Probing the molecular basis of substrate specificity, stereospecificity, and catalysis in the class II pyruvate aldolase, BphI. *Biochemistry 50*, 3559−3569.
(13) Carere, J., Baker, P., and Seah, S. Y. (2011) Investigating the molecular determinants for substrate channeling in BphI-BphJ, an aldolase-dehydrogenase complex from the polychlorinated biphenyls degradation pathway. *Biochemistry 50*, 8407−8416.
(14) Lee, S. J., Ko, J. H., Kang, H. Y., and Lee, Y. (2006) Coupled expression of MhpE aldolase and MhpF dehydrogenase in *Escherichia coli*. *Biochem. Biophys. Res. Commun. 346*, 1009−1015.
(15) Platt, A., Shingler, V., Taylor, S. C., and Williams, P. A. (1995) The 4-hydroxy-2-oxovalerate aldolase and acetaldehyde dehydrogenase (acylating) encoded by the nahM and nahO genes of the naphthalene catabolic plasmid pWW60-22 provide further evidence of conservation of meta-cleavage pathway gene sequences. *Microbiology 141* (Part 9), 2223−2233.
(16) Ling, H. B., Wang, G. J., Li, J. E., and Tan, H. R. (2008) sanN encoding a dehydrogenase is essential for nikkomycin biosynthesis in *Streptomyces ansochromogenes*. *J. Microbiol. Biotechnol. 18*, 397−403.
(17) Ling, H., Wang, G., Tian, Y., Liu, G., and Tan, H. (2007) SanM catalyzes the formation of 4-pyridyl-2-oxo-4-hydroxyisovalerate in nikkomycin biosynthesis by interacting with SanN. *Biochem. Biophys. Res. Commun. 361*, 196−201.
(18) Sambrook, J., Fritsch, E. F., and Maniatis, T. (1989) *Molecular cloning: A laboratory manual*, Cold Spring Harbor Laboratory Press, Plainview, NY.
(19) Yokoyama, S., Hirota, H., Kigawa, T., Yabuki, T., Shirouzu, M., Terada, T., Ito, Y., Matsuo, Y., Kuroda, Y., Nishimura, Y., Kyogoku, Y., Miki, K., Masui, R., and Kuramitsu, S. (2000) Structural genomics projects in Japan. *Nat. Struct. Biol. 7* (Suppl.), 943−945.
(20) Liu, H., and Naismith, J. H. (2008) An efficient one-step site-directed deletion, insertion, single and multiple-site plasmid mutagenesis protocol. *BMC Biotechnol. 8*, 91.
(21) Thompson, J. D., Gibson, T. J., and Higgins, D. G. (2002) Multiple sequence alignment using ClustalW and ClustalX. *Current Protocols in Bioinformatics*, Chapter 2, Unit 2, p 3, Wiley, New York.
(22) Manjasetty, B. A., Powlowski, J., and Vrielink, A. (2003) Crystal structure of a bifunctional aldolase-dehydrogenase: Sequestering a reactive and volatile intermediate. *Proc. Natl. Acad. Sci. U.S.A. 100*, 6992−6997.
(23) Armon, A., Graur, D., and Ben-Tal, N. (2001) ConSurf: An algorithmic tool for the identification of functional regions in proteins by surface mapping of phylogenetic information. *J. Mol. Biol. 307*, 447−463.
(24) Ashkenazy, H., Erez, E., Martz, E., Pupko, T., and Ben-Tal, N. (2010) ConSurf 2010: Calculating evolutionary conservation in sequence and structure of proteins and nucleic acids. *Nucleic Acids Res. 38*, W529−W533.
(25) DeLano, W. L. (2002) *The PyMOL Molecular Graphics System*, DeLano Scientific, San Carlos, CA.
(26) Krissinel, E., and Henrick, K. (2007) Inference of macromolecular assemblies from crystalline state. *J. Mol. Biol. 372*, 774−797.
(27) Jones, D. T., Taylor, W. R., and Thornton, J. M. (1992) The rapid generation of mutation data matrices from protein sequences. *Comput. Appl. Biosci. 8*, 275−282.
(28) Tamura, K., Peterson, D., Peterson, N., Stecher, G., Nei, M., Kumar, S. (2011)2011MEGA5: Molecular Evolutionary Genetics Analysis using Maximum Likelihood, Evolutionary Distance, and Maximum Parsimony MethodsMol. Biol. Evol.
(29) Bradford, M. M. (1976) A rapid and sensitive method for the quantitation of microgram quantities of protein utilizing the principle of protein-dye binding. *Anal. Biochem. 72*, 248−254.
(30) Cornish-Bowden, A. (1995) *Analysis of enzyme kinetic data*, Oxford University Press, New York.
(31) Jain, E., Bairoch, A., Duvaud, S., Phan, I., Redaschi, N., Suzek, B. E., Martin, M. J., McGarvey, P., and Gasteiger, E. (2009) Infrastructure for the life sciences: Design and implementation of the UniProt website. *BMC Bioinf. 10*, 136.
(32) Eaton, R. W. (1996) p-Cumate catabolic pathway in *Pseudomonas putida* Fl: Cloning and characterization of DNA carrying the cmt operon. *J. Bacteriol. 178*, 1351−1362.
(33) Zylstra, G. J., McCombie, W. R., Gibson, D. T., and Finette, B. A. (1988) Toluene degradation by *Pseudomonas putida* F1: Genetic organization of the tod operon. *Appl. Environ. Microbiol. 54*, 1498−1503.
(34) Powlowski, J., Sahlman, L., and Shingler, V. (1993) Purification and properties of the physically associated meta-cleavage pathway enzymes 4-hydroxy-2-ketovalerate aldolase and aldehyde dehydrogenase (acylating) from *Pseudomonas* sp. strain CF600. *J. Bacteriol. 175*, 377−385.
(35) Franklin, F. C., Bagdasarian, M., Bagdasarian, M. M., and Timmis, K. N. (1981) Molecular and functional analysis of the TOL plasmid pWWO from *Pseudomonas putida* and cloning of genes for the entire regulated aromatic ring meta cleavage pathway. *Proc. Natl. Acad. Sci. U.S.A. 78*, 7458−7462.
(36) Habe, H., Kasuga, K., Nojiri, H., Yamane, H., and Omori, T. (1996) Analysis of cumene (isopropylbenzene) degradation genes from *Pseudomonas fluorescens* IP01. *Appl. Environ. Microbiol. 62*, 4471−4477.
(37) Arai, H., Ohishi, T., Chang, M. Y., and Kudo, T. (2000) Arrangement and regulation of the genes for meta-pathway enzymes required for degradation of phenol in *Comamonas testosteroni* TA441. *Microbiology 146* (Part 7), 1707−1715.
(38) Ferrandez, A., Garcia, J. L., and Diaz, E. (1997) Genetic characterization and expression in heterologous hosts of the 3-(3-hydroxyphenyl)propionate catabolic pathway of *Escherichia coli* K-12. *J. Bacteriol. 179*, 2573−2581.
(39) Omokoko, B., Jantges, U. K., Zimmermann, M., Reiss, M., and Hartmeier, W. (2008) Isolation of the phe-operon from *G. stearothermophilus* comprising the phenol degradative meta-pathway genes and a novel transcriptional regulator. *BMC Microbiol. 8*, 197.
(40) Van der Geize, R., Yam, K., Heuser, T., Wilbrink, M. H., Hara, H., Anderton, M. C., Sim, E., Dijkhuizen, L., Davies, J. E., Mohn, W. W., and Eltis, L. D. (2007) A gene cluster encoding cholesterol catabolism in a soil actinomycete provides insight into *Mycobacterium tuberculosis* survival in macrophages. *Proc. Natl. Acad. Sci. U.S.A. 104*, 1947−1952.
(41) Furukawa, K., Hirose, J., Suyama, A., Zaiki, T., and Hayashida, S. (1993) Gene components responsible for discrete substrate specificity in the metabolism of biphenyl (bph operon) and toluene (tod operon). *J. Bacteriol. 175*, 5224−5232.
(42) Baker, P., and Seah, S. Y. (2012) Rational Design of Stereoselectivity in the Class II Pyruvate Aldolase BphI. *J. Am. Chem. Soc. 134*, 507−513.
(43) Dunn, M. F., Aguilar, V., Brzovic, P., Drewe, W. F. Jr., Houben, K. F., Leja, C. A., and Roy, M. (1990) The tryptophan synthase bienzyme complex transfers indole between the α- and β-sites via a 25−30 Å long tunnel. *Biochemistry 29*, 8598−8607.
(44) Miles, E. W. (1979) Tryptophan synthase: Structure, function, and subunit interaction. *Adv. Enzymol. Relat. Areas Mol. Biol. 49*, 127−186.
(45) Hettwer, S., and Sterner, R. (2002) A novel tryptophan synthase β-subunit from the hyperthermophile *Thermotoga maritima*. Quaternary

structure, steady-state kinetics, and putative physiological role. *J. Biol. Chem. 277*, 8194−8201.
(46) Leopoldseder, S., Hettwer, S., and Sterner, R. (2006) Evolution of multi-enzyme complexes: The case of tryptophan synthase. *Biochemistry 45*, 14111−14119.
(47) Ramani, A. K., and Marcotte, E. M. (2003) Exploiting the co-evolution of interacting proteins to discover interaction specificity. *J. Mol. Biol. 327*, 273−284.
(48) Fryxell, K. J. (1996) The coevolution of gene family trees. *Trends Genet. 12*, 364−369.
(49) Pages, S., Belaich, A., Belaich, J. P., Morag, E., Lamed, R., Shoham, Y., and Bayer, E. A. (1997) Species-specificity of the cohesin-dockerin interaction between *Clostridium thermocellum* and *Clostridium cellulolyticum*: Prediction of specificity determinants of the dockerin domain. *Proteins 29*, 517−527.
(50) van Kesteren, R. E., Tensen, C. P., Smit, A. B., van Minnen, J., Kolakowski, L. F., Meyerhof, W., Richter, D., van Heerikhuizen, H., Vreugdenhil, E., and Geraerts, W. P. (1996) Co-evolution of ligand-receptor pairs in the vasopressin/oxytocin superfamily of bioactive peptides. *J. Biol. Chem. 271*, 3619−3626.